Solid-State NMR Strategies for the Structural Investigation of Carbon-Based Anode Materials

Sophia Hayes, Leo van Wüllen, and Hellmut Eckert*

Department of Chemistry, University of California, Santa Barbara, California 93106

William R. Even and Robert W. Crocker

Sandia National Laboratories, P.O. Box 969, Livermore, California 94551

Zhengming Zhang

Eveready Battery Company, Inc., P.O. Box 45077, Westlake, Ohio 44145

Received July 22, 1996. Revised Manuscript Received January 2, 1997[⊗]

Multinuclear solid-state NMR spectroscopy is a well-suited technique for structural analysis of amorphous carbon-based anode materials generated from pyrolysis of poly(methacrylonitrile/divinylbenzene) copolymers. Results are presented for the untreated polymeric precursor, the oxidatively stabilized material, and amorphous carbons prepared by high-temperature pyrolysis. In addition, structural effects of silicon dopants and lithium intercalants are studied. The structural changes occurring during the processes of oxidative stabilization and carbonization up to 700 °C are effectively monitored by ^{13}C and ^{15}N cross-polarization/magic angle spinning methods. The peak assignments are assisted by short contact time and dipolar dephasing experiments. For carbons prepared at higher pyrolysis temperatures this technique is limited by the low structural proton content. For such materials, the ^{1}H chemical shifts of sorbed water molecules are found to be linearly correlated with the pyrolysis temperature. This effect is attributed to surface ordering phenomena. ^{29}Si CPMAS spectra of carbons prepared with tetravinylsilane comonomers indicate that the silicon component is oxidized during the stabilization process. ^{7}Li MAS NMR is well suited to differentiate between electrochemically relevant intercalated species and other species that are unable to participate in the intercalation due to parasitic processes. For the intercalated species, a linear correlation of the ^{7}Li chemical shift with the charging state of the carbon is observed.

Introduction

Because of their chemical stability and relative inertness, lithium−graphite intercalation compounds have garnered considerable interest as a substitute for metallic lithium or lithium alloy-based anodes in rechargeable solid electrolyte batteries.[1,2] Such intercalated LiC_n systems can tolerate more than 1000 deep charge−discharge cycles.[3] To date, the significant drawback of these materials has been the low lithium utilization ratio, Li:C, which is limited by the stoichiometry of the graphitic intercalation compound represented by LiC_6 or 372 mAh/g.[4] Recently, disordered and turbostratic (random stacking) carbon materials have become a focus of interest, because they appear to allow for significantly higher intercalation levels; claims ranging up to the composition LiC_2 have been reported.[5] Furthermore, lithium intercalation into these materials is associated with virtually no change in interlayer spacing, resulting in less microstructural distortion during cycling and better reversibility. The excellent cycling behavior, which is superior to that of metallic lithium anodes, can be attributed to the stabilization of an expanded lattice parameter in these disordered materials relative to the spacing observed after lithium insertion into graphite.

Most of the disordered carbons used for these purposes are prepared by pyrolysis of organic polymer precursors within the temperature range 400−1100 °C. X-ray diffraction and electron microscopy results indicate that many of these materials are composed primarily of domains where the carbon is considerably disordered within which randomly stacked ordered domains, sometimes termed turbostratic, are observed.

Previous studies have shown that emulsion derived copolymers of poly(acrylonitrile/divinylbenzene) (PAN/DVB) and poly(methylacrylonitrile/ divinylbenzene) (PMAN/DVB) are stable, highly cross-linked systems and can serve as suitable carbon precursors.[6] Figure 1

[⊗] Abstract published in *Advance ACS Abstracts,* February 15, 1997.

(1) Yazami, R.; Touzain, Ph. *J. Power Sources* **1983**, *9*, 365.

(2) (a) Billaud, D.; Henry, F. X.; Willmann, P. *Mater. Res. Bull.* **1993**, *28*, 477. (b) Billaud, D.; Henry, F. X.; Willmann, P. *Mol. Cryst. Liq. Crest.* **1994**, *245*, 159.

(3) Besenhard, J. O. *Progress in Intercalation Research*; Müller-Warmuth, W., Schöllhorn, R., Eds.; Kluwer Academic Publishers: Dordrecht, 1994; pp 457−508.

(4) (a) Basu, S.; Zeller, C.; Flanders, P. J.; Fuerst, C. D.; Johnson, W. D.; Fischer, J. E. *Mater. Sci. Eng.* **1979**, *38*, 275. (b) Guerard, D.; Herold, A. *Carbon* **1975**, *13*, 337. (c) Woo, K. C.; Mertwoy, H.; Fischer, J. E.; Kamitakahara, W. A.; Robinson, D. S. *Phys. Rev. B* **1983**, *27*, 7831.

(5) (a) Yazami, R.; Cherigui, A.; Nalimova, V. A.; Guerard, D. *Proc. Symp. Lithium Batteries*; Surampudi, S., Koch, V. R., Eds.; The Electrochemical Society: Pennington, NJ, 1993; Vol. 24, p 1. (b) Imoto, H.; Omaru, A.; Azuma, H.; Nishi, Y. *Ibid.*, p 9. (c) Huang, C. K.; Surampudi, S.; Attia, A.; Halpert, G. *Ibid.*, p 32. (d) Takami, N.; Sato, A.; Ohsaki, T. *Ibid.*, p 44. (e) Dahn, J. R.; Sleigh, A. K.; Shi, H.; Reimers, J. N.; Zhong, Q.; Way, B. M. *Electrochim. Acta* **1993**, *38*, 1179.

S0897-4756(96)00389-4 CCC: $14.00

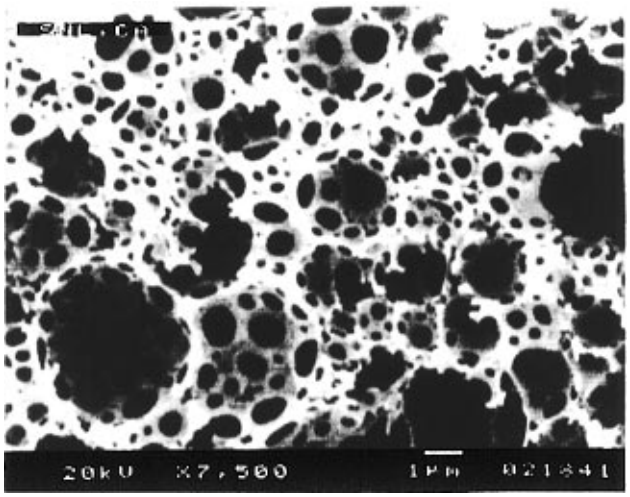

Figure 1. Scanning electron micrograph of an emulsion-derived PMAN/DVB foam, 1/1 mole ratio MAN/DVB, pyrolyzed at 1100 °C.

shows a typical SEM photograph, revealing the high porosity of one such material. The carbons derived from the pyrolysis of these materials are being studied for air separation, catalysis, and battery anode applications. Their preparation is carried out in a three-step process: (1) polymerization of the monomers in an inverse micelle emulsion, (2) oxidative stabilization by treatment in air at temperatures near 200−250 °C, and (3) pyrolysis within the temperature range 400−1100 °C.

During the oxidative stabilization of these materials, prior to carbonization/ pyrolysis, important structural changes take place which have lasting effects on the end products.[7] These changes influence not only the stability of the decomposition intermediates (and hence affect the char yield) but also the eventual ability and extent of lithium intercalation. Unlike the situation in polyacrylonitrile (PAN), the literature is conspicuously sparse concerning the structural transformation during this stabilization process for PMAN. Likewise, little is known about the structural changes occurring during the high-temperature pyrolysis or the effect of the resulting microstructure on the intercalation process. Specifically, the role of matrix atoms other than carbon remains unexplored. This statement applies to both intrinsic species such as the nitrogen and hydrogen atoms introduced into the matrix from the polymer precursors, as well as extrinsic species such as the oxygen incorporated during the stabilization. Other extrinsic species or codopants such as silicon or boron are occasionally introduced into the matrix with the goal of enhancing material performance.[8] Finally, the local environments and spatial organization of the lithium ions are of great importance both for their scientific merit and impact on cell design applications in the commercial battery arena. Figure 2 illustrates schematically the various possible lithium environments that might be produced during electrochemical intercalation of a porous carbon electrode. Several possible lithium destinations include intercalation into small, locally ordered stacks of graphitic-like layers (in analogy with formation of the graphite intercalation compound, LiC_6) or in turbostratic regions of disordered stacks. Within these disordered regions, the first coordination sphere of the Li atoms might contain, besides carbon atoms, residual nitrogen or hydrogen atoms also introduced from the precursor, and/or oxygen atoms introduced by the stabilization process. Alternatively, the intercalation process has been proposed to involve the formation of Li dimers[9] or small clusters within defects or microstructural voids. All these environments comprise electrochemically relevant lithium species. In addition to these reversibly occupied sites, there may be irreversibly formed, ionic lithium compounds such as LiOH, Li_2CO_3, or Li polycarbonates produced at the surface, arising from parasitic passivation processes (i.e., electrochemical decomposition of the organic electrolyte), or even surface-adsorbed lithium transport salts from the electrolyte solution.

Several types of disordered carbons reversibly intercalate lithium in excess of the graphitic stoichiometry of LiC_6. To verify the enhanced intercalation levels within this class of carbons, it is important to differentiate between the electrochemically relevant lithium species that are truly reversibly intercalated and those lost to traps, such as those located in the passivation layer or associated with structural "lattice defects" within the solid-state microstructure. Altogether, at each stage of material synthesis, the materials issues described above represent a host of possibilities focusing on the relationship between microstructure and performance. These need to be addressed by suitable experimental techniques. Being an element-selective, inherently quantitative method sensitive to local environments, solid-state nuclear magnetic resonance (NMR) represents an ideal structural tool for addressing questions of the kind identified above.[10] A variety of selective techniques are available, allowing intricate structural detail to be resolved, frequently by means of special isotopically labeled synthesis, by combining complementary experiments, and by monitoring the dependence of the spectra on parameters relating to material composition and processing history.

NMR studies on graphite and graphite-related materials are intrinsically difficult. The low natural abundance (1%) of the NMR-active isotope ^{13}C and its moderately low gyromagnetic ratio (γ) pose limitations on the detection sensitivity. Additional complications arise from probe detuning effects due to the considerable electrical conductivity of the materials. The latter problem can be alleviated by the use of inert filler materials, yet at the expense of detection sensitivity. High-resolution ^{13}C and ^{15}N NMR spectra are most conveniently obtained using magnetization transfer ("cross-polarization") between the abundant proton and the dilute heteronuclear spin systems. While this technique works satisfactorily with the polymeric precursors, it may produce nonrepresentative spectra or even fail altogether for pyrolyzed materials very dilute in residual hydrogen, such as the amorphous carbons when produced at temperatures above 500 °C (see below). In these cases, it is necessary to resort to simple

(6) Even, W. R.; Gregory, D. P. *MRS Bull.* **1994**, *19*, 29.
(7) (a) Fitzer, E.; Frohs, W.; Heine, M. *Carbon* **1986**, *24*, 387. (b) Memetea, L. T.; Billingham, N. C.; Then, E. T. H. *Polym. Degrad. Stab.* **1995**, *47*, 189.
(8) Wilson, A. M.; Way, B. M.; Dahn, J. R.; van Buuren, T. *J. Appl. Phys.* **1995**, *77*, 2363.
(9) Sato, K.; Noguchi, M.; Demachi, A.; Oki, N.; Endo, M. *Science* **1994**, *264*, 556.
(10) Eckert, H. *Prog. NMR Spectrosc.* **1992**, *24*, 159.

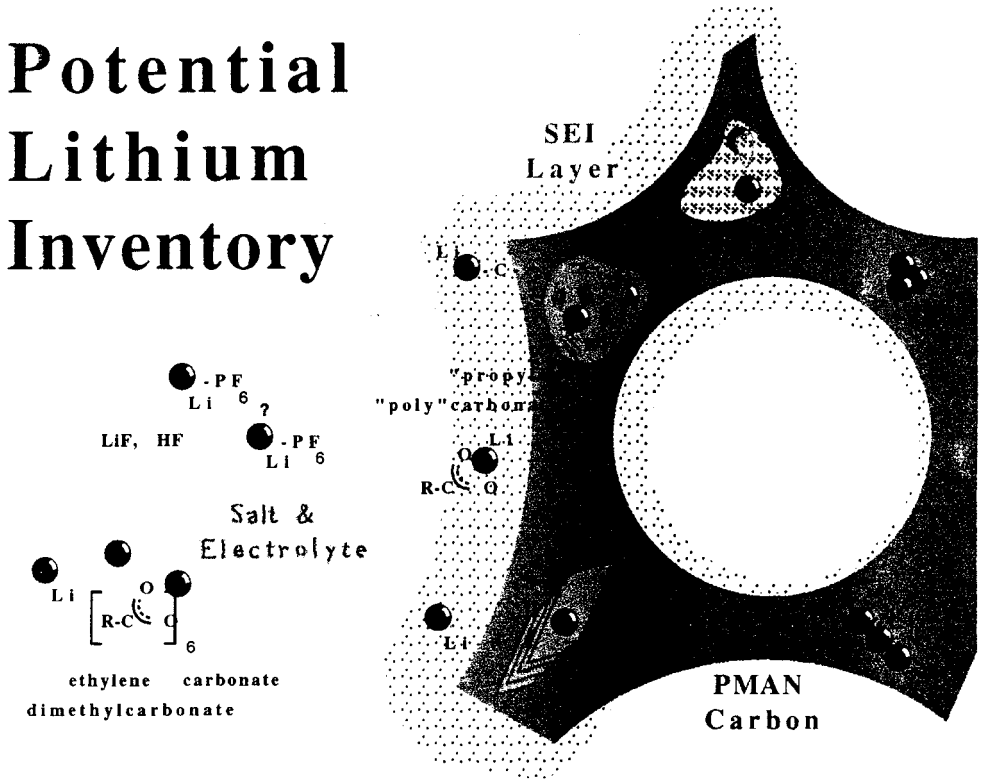

Figure 2. Graphical depiction of possible lithium sites in the carbon foam.

Bloch decay methods for recording solid-state NMR spectra. The chemical environments of the residual surface protons in these materials may be characterized further by ^{1}H magic angle spinning NMR. As reported previously, amorphous carbon pyrolysates also tend to sorb moisture from the atmosphere, and the chemical environments sampled by these water molecules within accessible surfaces are sensitively reflected by the chemical shifts recorded in such measurements.[11] Finally, the extent of charge-transfer and guest−host interactions in lithium intercalation compounds can be estimated from measurements of the ^{7}Li chemical shifts. This has been demonstrated previously in the NMR studies of lithium−graphite intercalation compounds[12] and, more recently, also for reaction products of lithium with less ordered carbons.[9,13] The present contribution serves to illustrate the utility, potential, and limitations of these complementary NMR approaches in characterizing the successive chemical conversions from the untreated polymer precursor to the final, active anode material.

Experimental Section

Sample Preparation and Characterization. Samples were prepared at Sandia National Laboratories, Livermore, using protocols previously reported.[6,14] This process involves the water-phase free radical polymerization of the monomer-containing oil phase in a surfactant-stabilized inverse emulsion system. The water phase represents the eventual pore-forming structure in the final porous product. The polymerization was carried out at 65 °C for 48 h in sealed polypropylene bottles, resulting in a highly cross-linked and completely insoluble material. The monomers, methacrylonitrile (MAN, reagent grade, purchased from Aldrich) and divinylbenzene (DVB, technical grade, purchased from Dow, a 90% mixture of o-, m-, and p-isomers with balance primarily ethylbenzene), were combined in a 1:1 volume ratio and mixed with a surfactant, sorbitan monoleate (SMO, purchased from Aldrich), and a water-based solution of an initiator, 0.04 M ammonium persulfate. The mixture was shaken vigorously in order to obtain a stable emulsion between the oil (monomer) phase and the water (initiator and temporary pore former). The emulsion was then put in a forced air oven at 65 °C cure. The cured material was removed from the bottles, dried, and finely ground, and finally the slurry was washed to remove the processing salts. The resulting product was a 1−5 μm, free-flowing powder. To study the influence of silicon-based codopants on the final carbon structure, a separate set of samples was prepared using tetravinylsilane (reagent grade, purchased from Aldrich). For assignment purposes, isotopically enriched ^{15}N and ^{2}H analogues (purchased from Cambridge Isotopes) were used to prepare polymers for each of the preparation stages. Homopolymer materials derived from pure methacrylonitrile and divinylbenzene were also synthesized by similar emulsion routes.

At a second stage of the preparation process, the copolymer powder was thermally and/or oxidatively "stabilized" using typical conditions summarized in ref 6. This was accomplished in a programmable, forced-air oven. The powder bed temperature was carefully maintained, and the controlled oxidation process was not allowed to thermally run away. This was most easily accomplished by keeping bed depth to less than 2 cm. After stabilization, the carbonization was carried out on both free-powder beds and disks pressed from the stabilized powder. Approximately 100 g of powder was placed in an alumina tray, while the disks were placed on graphite plates and inserted into a three-zone, 6 in. tube furnace. The furnace was equipped with gas-tight endplates which allowed control over the internal atmosphere. Pyrolysis occurred in an argon

(11) Eckert, H.; Levendis, Y. A.; Flagan, R. C. *J. Phys. Chem.* **1988**, *92*, 5011.

(12) (a) Carver, G. P. *Phys. Rev. B* **1970**, *2*, 2284. (b) Conard, J.; Estrade, H. *Mater. Sci. Eng.* **1977**, *31*, 173. (c) Müller-Warmuth, W. *Progress in Intercalation Research*; Müller-Warmuth, W., Schöllhorn, R., Eds.; Kluwer Academic Publishers: Dordrecht, 1994; p 339−455.

(13) Mori, Y.; Iriyama, T.; Hashimoto, T.; Yamazaki, S.; Kawakami, F.; Shiroki, H.; Yamabe, T. J. *Power Sources* **1995**, *56*, 205.

(14) (a) Barby, D.; Haq, Z. U.S. Patent No. 4,552,953, (1985). (b) Haq, Z. U.S. Patent No. 4,536,521, (1985). (c) Jones, K.; Lothian, B.; Martin, A.; Taylor, G.; Haq, Z. U.S. Patent No. 4,611,014, (1986).

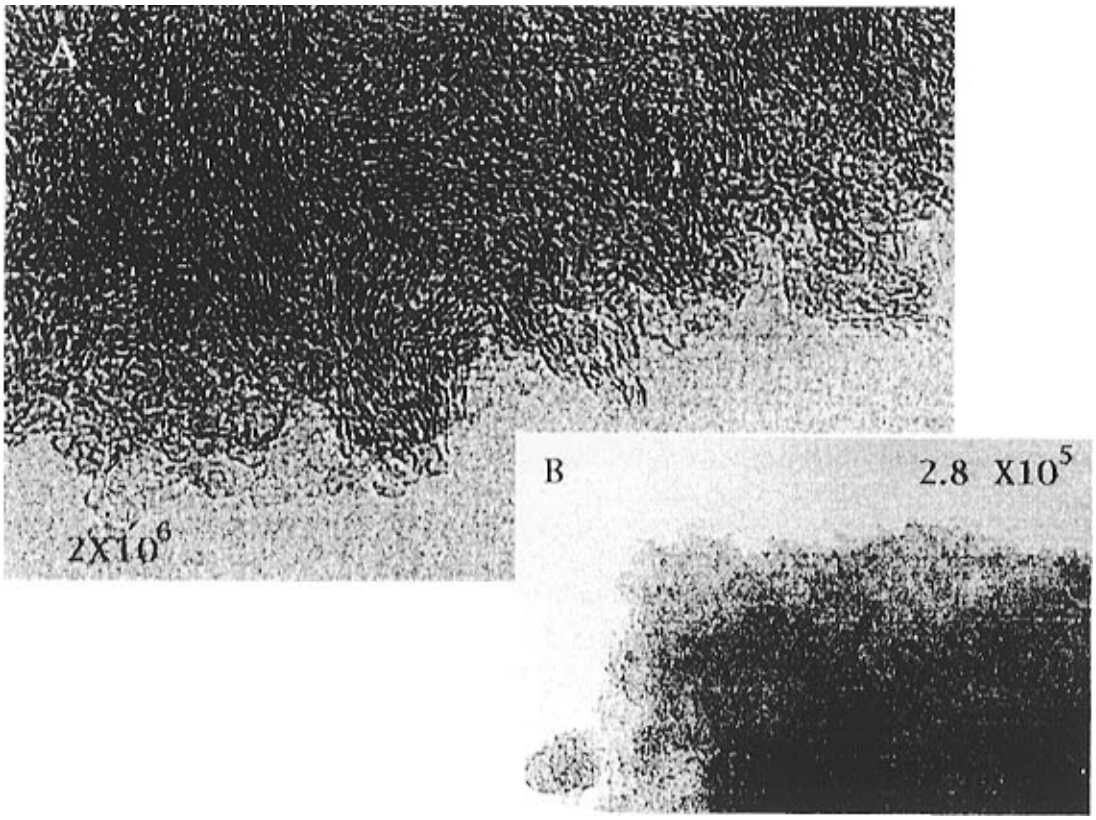

Figure 3. Transmission electron micrograph of a PMAN homopolymer derived carbon pyrolyzed at 1000 °C. Very small regions of parallel stacking can be seen in the carbon interior (see part A); while at lower magnification, inset B demonstrates that domains of differing density exist within the general carbon mass. Numbers indicate magnification.

atmosphere, at final temperatures ranging between 400 and 1100 °C; the materials were exposed to the upper temperature limit for either 20 min or allowed to reach equilibrium at 5 h.

Both X-ray and TEM analysis of the final carbon indicated that the material was extensively disordered, without any indication of long-range order (see Figure 3). Elemental analysis indicated that the materials were >90 wt % carbon with N, O, and H residuals decreasing with elevated temperature exposure. Materials prepared at low temperatures, 500 °C, are microporous with surface areas in excess of 150 m^2/g. As the pyrolysis temperature increases, the surface area drops to values on the order of 20−50 m^2/g.

The intercalation was performed at Eveready Battery Co. for Sandia. Lithium intercalated samples of the pyrolyzed carbons were prepared for electrochemical testing in an argon glovebox, and extreme care was taken to exclude oxygen and water. The electrolyte was 1 M $LiPF_6$ in a mixed ethylene carbonate/diethyl carbonate solvent (1:1 volume ratio). The test cell consisted of a working electrode made from a carbon foam pellet without binder and counter and reference electrodes of lithium metal.

The carbon electrodes were cycled by constant current lithiation and delithiation at 0.5 mA/cm^2 and 25 °C. The cycling potential ranged from 3.0 to 0.0 V versus lithium. Samples were cycled between fully intercalated and deintercalated stages in excess of 10 cycles to ensure steady-state processes. At this point, no additional lithium losses were observed to parasitic processes, and the reversible cycle-to-cycle efficiency was greater than 99%. In all cases, intercalation levels greater than 450 mAh/g were achieved.

Solid-State NMR. Unless noted otherwise, all of the NMR experiments were undertaken on a General Electric GN-300 spectrometer equipped with 7 mm multinuclear magic angle spinning (MAS) NMR probes from Doty Scientific. MAS spinning speeds ranged typically between 3 and 7 kHz. ^{13}C cross-polarization (CP) experiments were conducted at 75 MHz using the following typical experimental parameters: spinning frequency 5 kHz, contact time 1 ms, ^1H 90° pulses of 5−7 μs length, relaxation delay 2−3 s. Spectral editing (see below) was accomplished by (1) measurements with very short contact times (20 μs), and (2) interrupted decoupling experiments using 350−450 μs dipolar dephasing periods. In the latter, phase distortions were avoided by recording a rotor-synchronized MAS spin−echo. Samples with hydrogen contents too low for cross polarization were examined by Bloch decay and static spin−echo studies. These experiments used 90° pulses of 7 μs length and relaxation delays of 10 s. In many cases probe detuning effects were overcome by dividing the material with approximately 50% (v/v) of NaCl filler material.

To probe the structural environments of the nitrogen species, a set of samples was prepared using ^{15}N-enriched methacrylonitrile. $^1H-^{15}N$ CPMAS NMR experiments were carried out using a Bruker AMX-500 spectrometer equipped with a Doty probe at 50.7 MHz using the following parameters: contact time 2 ms, ^1H 90° pulse length 7.2 μs, relaxation delay 2 s. Conditions for cross-polarization were optimized on a sample of ^{15}N-labeled glycine, which also served as a secondary reference material with respect to nitromethane (CH_3NO_2).

The structural environment of silicon dopants was explored on samples copolymerized with tetravinylsilane, using a Chemagnetics CMX 500 NMR spectrometer. Parameters for $^1H-^{29}Si$ CPMAS NMR were resonance frequency 99.06 MHz, contact time 5 ms, ^1H 90° pulse length 8.5−11 μs, relaxation delay 4−5 s. ^1H MAS NMR experiments were carried out at 300.56 MHz, using a typical spinning speed of 5 kHz, 90° pulses of 4−7 μs length, and relaxation delays of 1−2 s. Lithium-intercalated samples were examined by ^7Li MAS NMR at 116.8 MHz with 90° pulses of 20 μs length, relaxation delays of 1−120 s (with 30 s being typical), and 3−4 kHz spinning speed. Chemical shifts of the ^1H, ^{13}C, and ^{29}Si resonances are reported against tetramethylsilane (TMS). The ^7Li chemical shifts are reported against a 1.0 M aqueous solution of LiCl.

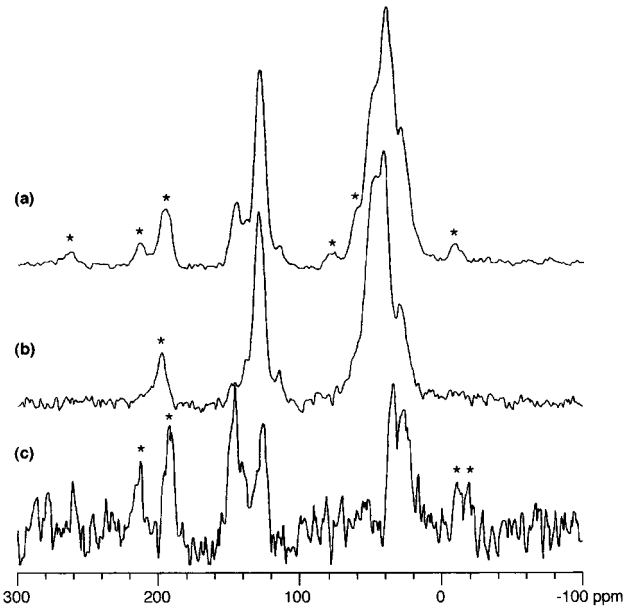

Figure 4. ^{13}C CPMAS NMR spectra of untreated PMAN/DVB: (a) contact time 1 ms; (b) contact time 20 μs; (c) interrupted decoupling. Spinning sidebands are indicated by asterisks.

Results and Discussion

In the presentation of the NMR results to follow, we will adhere to the sequence followed in the preparation of the materials studied, i.e., (1) characterization of the untreated polymer samples, (2) structural effects of thermal/oxidative stabilization, (3) conversion of the stabilized polymer precursor to amorphous carbon, and (4) the effect of silicon codopants and lithium intercalation.

(1) Untreated Polymer Samples. Figure 4a shows ^{13}C CPMAS NMR results of untreated poly(methacrylonitrile/divinylbenzene) (PMAN/DVB) copolymer. The spectrum shows a large peak cluster centered in the 115−145 ppm range, representing aromatic (and possibly olefinic) carbon environments and the resonance due to the nitrile group. A second peak cluster in the 20−50 ppm range arises from diverse aliphatic carbon species. Peak assignments were accomplished by specific spectral editing experiments, the results of which are included in Figure 4: Since the rate of ^{13}C magnetization buildup increases with increasing strength of the $^{1}H-^{13}C$ dipole−dipole coupling, the resonances arising from protonated C atoms are selectively enhanced by CP experiments with very short contact times (Figure 4b). On the other hand, the resonances arising from such species can be suppressed selectively by preceding the signal acquisition with a delay during which the ^{1}H decoupler is turned off ("interrupted decoupling"), causing the transverse magnetization of rigid protonated C atoms to dephase rapidly in the dipolar fields of the surrounding ^{1}H spins. As a consequence, only the resonances of quaternary C atoms are detected, as well as the methyl resonances in which the $^{1}H-^{13}C$ dipolar interactions are partially averaged out by the rapid reorientation around the 3-fold axis (Figure 4c). On the basis of these experiments as well as the NMR spectra of the neat homopolymers the complete peak assignments are summarized in Table 1. Results for the poly-DVB and poly-MAN homopolymers are in good agreement with those reported in the literature.[15,16] Additional experiments were undertaken on copolymerisates, in which the DVB component was fully deuterated. The ^{13}C CPMAS spectra are shown in Figure 5. This experiment allows the resonance assignment for the aliphatic C atoms in the spectra shown (see Table 1). Furthermore, Figure 5 demonstrates the ability of cross-polarizing the deuterated C atoms of the DVB component from the ^{1}H nuclei of the PMAN component. This result indicates intimate or random mixing of both repeat units in the copolymer precursor rather than segmentally mixed blocks of homopolymer runs. Finally, the ^{15}N CPMAS NMR spectrum (Figure 6a) reveals a single site at −128 ppm with a spinning sideband pattern indicative of an axially symmetric chemical shielding tensor. This result is consistent with the published solid-state ^{15}N NMR of nitrile groups in solids[17] and indicates that in the present material the nitrile group fully preserves

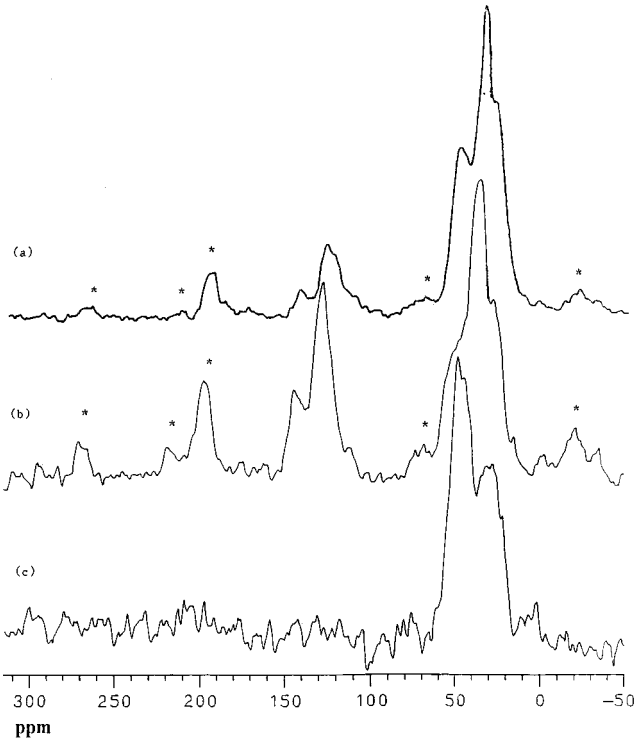

Figure 5. ^{13}C CPMAS NMR spectra of untreated PMAN/(d-DVB): (a) contact time 1 ms; (b) interrupted decoupling; (c) contact time 20 μs. Spinning sidebands are indicated by asterisks.

Table 1. PMAN/DVB Peaks

peaks (ppm)	description	assignment
27.5	shoulder	methyl group
29.4−29.8	medium,sharp	methyl group
34.1	shoulder	quaternary C
40.4−41.5	large, sharp	methylene (DVB)
47.2	shoulder	methylene (MAN)
114.5−114.7	small	vinyl group (residual)
125.7	slight shoulder	aromatic bridgehead (nonprotonated)
128.4−128.9	large, sharp	aromatic (protonated)
approximately 140	small	nonprotonated aromatic group
144.7−145.3	medium, sharp	aromatic bridgehead (nonprotonated)

(15) Kawamura, T.; Toshima, N.; Matsuzaki, K. *Macromol. Chem. Phys.* **1994**, *195*, 3343.

(16) Law, R. V.; Dennison, P. R.; Snape, C. E.; Sherrington, D. C. *Am. Chem. Soc. (Div. Polym. Chem., Polym. Prepr.)* **1993**, *34*, 558.

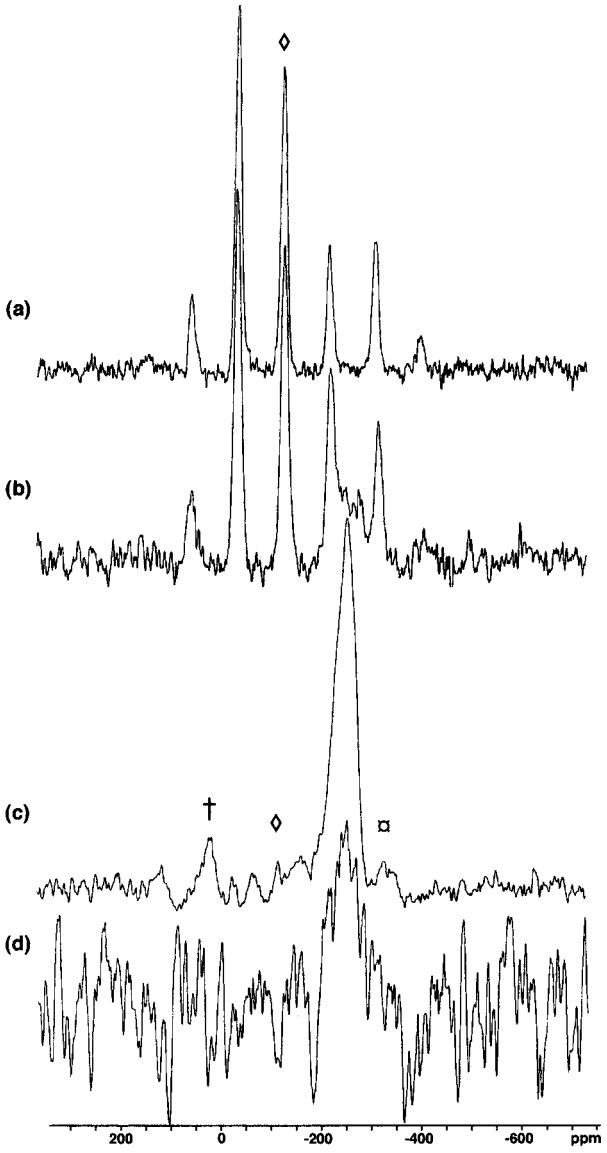

Figure 6. ^{15}N CPMAS NMR data of labeled poly(^{15}N-MAN)/DVB materials: (a) untreated; (b) oxidatively stabilized; (c) carbonized, 500 °C; (d) carbonized, 700 °C. Symbols (◇, ○, †) denote central MAS peaks.

its structural integrity under the polymerization conditions.

(2) Thermally/Oxidatively Stabilized Samples. The oxidative stabilization process is an essential step in the preparation of the carbons. As shown empirically, heating the copolymers in air according to specific time/temperature protocols helps the material maintain a stable morphology and surface structure and prevents melting and coking during pyrolysis. As a consequence, the char yield in the final product is greatly enhanced. Unlike other systems, e.g., polyacrylonitrile (PAN), the PMAN/DVB material itself does not undergo appreciable shrinkage or mass loss and exhibits only a minor color change from white to light beige; however, the actual chemical changes occurring during this process are unknown. On the basis of substantially more experimental evidence, various mechanisms have been proposed for the stabilization of the related polyacrylonitrile (PAN) and its fibers.[7] Generally for PAN, these proposals invoke cyclization of the nitrile group, resulting in increased aromatization and participation of nitrogen in heterocyclic structures. Because of the highly cross-linked nature of PMAN/DVB, such "wholesale" reorganization is not likely to occur due to the severely limited mobility of the segments between cross-links. To assess the influence of the stabilization protocol on the present materials, the same ^{13}C CPMAS protocol was applied that was used for the corresponding untreated polymer precursors. Figure 7 depicts the results for the PMAN/DVB copolymer. Comparison of Figure 7 with the spectra of the untreated polymer precursors reveals only minor changes in peak intensity and shifts, indicating nearly complete retention of the basic polymer structure during the oxidative treatment. Nevertheless, the appearance of a new spectral feature at 168 ppm, most clearly seen in the interrupted decoupling experiments, indicates formation of a distinct new species in all the samples. The chemical shift of this resonance is most consistent with a carboxyl, ester, or amide group.[18] We attribute this unit primarily to carboxylic acid (or possibly ester) -like moieties formed by the oxidation of dangling vinyl groups. This assignment is based on the fact that a similar peak is present in stabilized poly-DVB (which is nitrogen-free). In view of the ^{15}N CPMAS results discussed below, it is also possible that amide groups contribute to spectral intensity in the 160−170 ppm region in the ^{13}C NMR spectrum of the oxidatively stabilized copolymer.

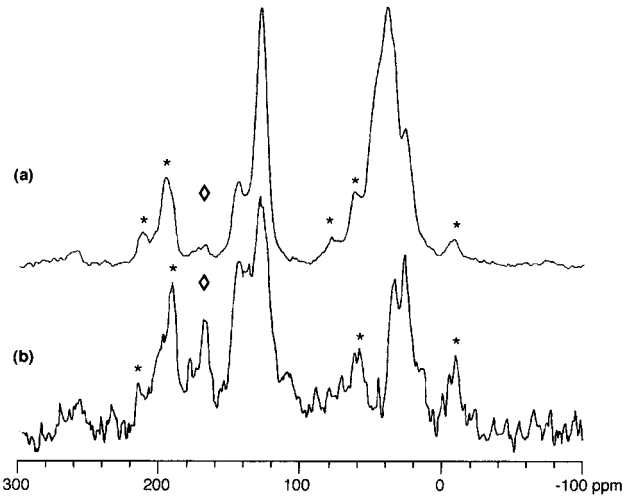

Figure 7. ^{13}C CPMAS NMR spectra of oxidatively stabilized PMAN/DVB: (a) contact time 1 ms; (b) interrupted decoupling. Spinning sidebands are indicated by asterisks. The symbol (◇) marks a new feature appearing after stabilization.

Minor aromatization of the PMAN component during the oxidative stabilization process is supported by subtle intensity changes in the aliphatic region of the CPMAS spectrum. More direct evidence for the chemistry occurring during the stabilization comes from the ^{15}N CPMAS spectrum (Figure 6b). Several different nitrogen environments can be discerned, of which that at −128 ppm can be assigned to a population of unaltered nitrile groups. The broad peak cluster within the region −250 to −290 ppm appears in the amide chemical shift

(17) Witanowski, M.; Stefaniak, L.; Webb, G. A. *Annual Reports on NMR Spectroscopy;* Webb, G. A., Ed.; Academic Press: New York, 1986; p 438.

(18) Hesse, M.; Meier, H.; Zeeh, B. *Spektroskopische Methoden in der organischen Chemie*; Georg Thieme Verlag: Leipzig, 1991; pp 137−200.

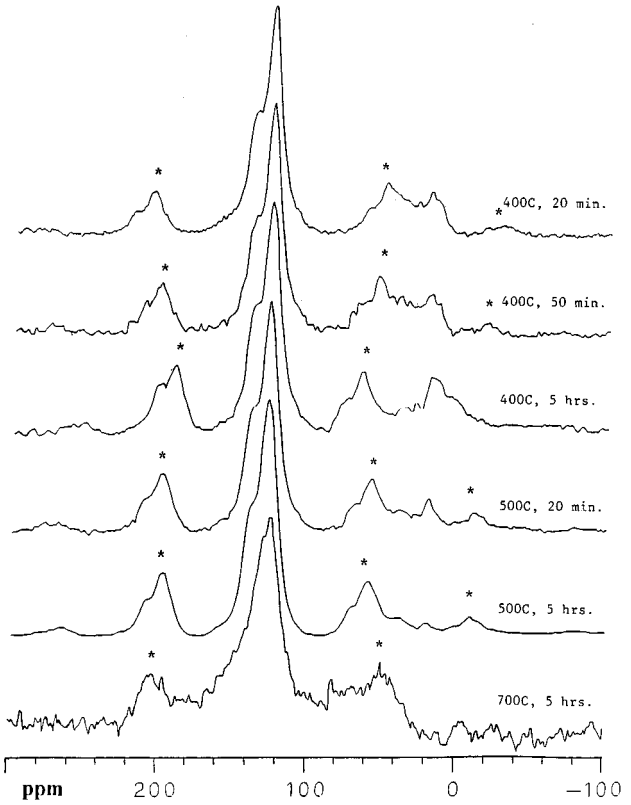

Figure 8. ^{13}C CPMAS NMR spectra of carbonized PMAN/DVB, pyrolyzed at various temperatures and times. Spinning sidebands are indicated by asterisks.

region. These chemical shifts are rather different from those expected for sp^2-hybridized nitrogen contained in imines or aromatic heterocyclic[19] species, which have been proposed to form via thermal cyclization in PAN.[7] Therefore, the results obtained here suggest that the thermal stabilization in PMAN/DVB proceeds via a different mechanism. The more limited cross-linking evident from our results is in agreement with previous conclusions concerning differences in the structural transformation of PMAN and PAN upon heat treatment.[20]

(3) Carbonized Materials. Conversion of the stabilized copolymer to an amorphous carbon material is critically affected by the duration, temperature, and surrounding atmosphere during pyrolysis. To assess the influence of these conditions, a variety of solid-state NMR parameters have been monitored. For example, Figure 8 shows the ^{13}C CPMAS spectra of the amorphous carbons as a function of pyrolysis time and temperature from 400 to 700 °C for a series of samples pyrolyzed in argon. With increasing degree of carbonization at higher and higher temperatures and longer times, fewer protons are available for cross-polarization, resulting in an overall signal-to-noise degradation, and the selective enhancement of C atoms near protons in the spectra. In addition, it becomes more difficult with these samples to optimize the experimental conditions for CPMAS since the high electrical conductivity leads to serious probe detuning effects. Finally, EPR experiments indicate a dramatic increase in paramagnetic spin concentrations as the pyrolysis temperature is increased. Due to all of these complications, the CP-MAS NMR spectra of the pyrolysates cannot necessarily be viewed as representative of the entire sample. With these caveats in mind, Figure 8 illustrates the general trend as a function of pyrolysis temperature. Treatment at 400 °C for only 20 min already results in the disappearance of most of the aliphatic carbon content, and only a small peak near 20 ppm reveals some residual CH_3 groups, which are associated with the MAN component. The remaining intense resonances in the 120−140 ppm region are due to various aromatic and olefinic carbon sites. The 140 ppm feature is much enhanced in the interrupted decoupling experiments, indicating nonprotonated carbon atoms. Pyrolysis at 500 °C results in spectra that are only slightly different (Figure 8), except for a further attenuation of the methyl resonance. For this pyrolysis temperature, the spectrum looks very similar to that of a pyrolyzed DVB homopolymer except for the absence of the methyl resonance in the latter (data not shown). The CPMAS spectra of the samples pyrolyzed at 700 °C (Figure 8, bottom) show significant peak broadening due to the presence of multiple aromatic carbon environments and possibly paramagnetic interactions. Here, the distribution of isotropic chemical shifts has become so wide that the ability of MAS to produce high-resolution spectra is severely compromised. This effect is even stronger for the Bloch decay spectra, which are essentially indistinguishable from those obtained by static NMR. Excessive line broadening effects of this kind have been observed previously in the NMR spectra of amorphous carbons prepared by radio frequency sputtering of graphite samples.[21] Figure 9 shows the static spectrum (obtained by a Hahn spin−echo sequence) of a sample pyrolyzed at 1000 °C. The line shape is characteristic of an axially symmetric chemical shift tensor with approximate components of 0 and 180 ppm parallel and

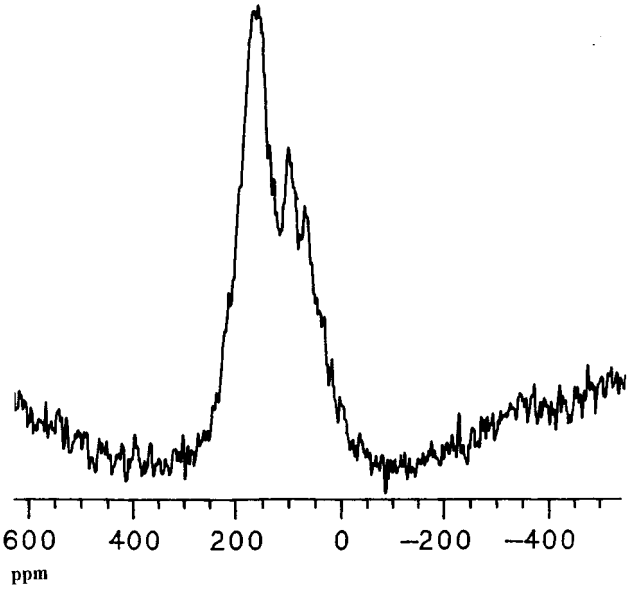

Figure 9. Static ^{13}C Hahn spin−echo spectrum of PMAN/DVB, pyrolyzed for 5 h at 1000 °C. Minor peaks near 76 and 109 ppm are from probe background.

(19) (a) Kaplan, S.; Pines, A.; Griffin, R. G.; Waugh, J. S. *Chem. Phys. Lett.* **1974**, *25*, 78. (b) Sardashti, M.; Maciel, G. E. *J. Phys. Chem.* **1988**, *92*, 4620.

(20) Kolarz, B. N.; Trochimczuk, A. W.; Wojaczynska, M.; Drewniak, M. *Angew. Makromol. Chem.* **1994**, *217*, 19.

(21) Pan, H.; Pruski, M.; Gerstein, B. C.; Li, F.; Lannin, J. S. *Phys. Rev. B* **1991**, *44*, 6741.

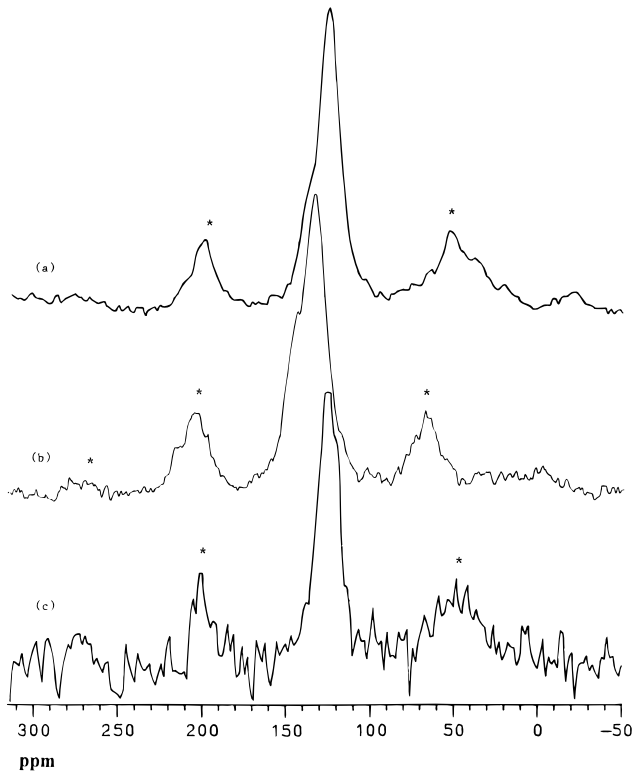

Figure 10. ^{13}C CPMAS NMR spectra of carbonized PMAN/(d-DVB), pyrolyzed at 500 °C for 5 h: (a) contact time 1 ms; (b) interrupted decoupling; (c) contact time 20 μs. Spinning sidebands are indicated by asterisks.

perpendicular to the principal axis. These parameters are similar to those observed for graphite,[22] suggesting a similar chemical environment of the nearest-neighbor coordination sphere.

Figure 10 shows the CPMAS NMR results of the PMAN/d-DVB sample pyrolyzed at 500 °C for 5 h. An interesting observation is that unlike the situation in the untreated and oxidatively stabilized PMAN/d-DVB copolymer, the spectrum of carbonized PMAN/d-DVB (i.e., a material in which all of the aromatic C atoms should be fully deuterated), nevertheless shows aromatic C atoms, which are directly bonded to hydrogen as the short-contact time experiment indicates (Figure 10c). There is a large fraction of directly protonated aromatic groups near 125 ppm, indicating either hydrogen exchange under the pyrolysis conditions or aromatic species arising from the cyclization of the aliphatic residues in the MAN component. Figure 6c shows the ^{15}N CPMAS spectrum of a ^{15}N-enriched sample pyrolyzed at 500 °C, revealing a dominant resonance at −253 ppm, and several other smaller resonances at +19, −119, and −328 ppm. The chemical shift of the dominant peak at −253 ppm is characteristic of nitrogen situated within amide groups. The assignment of these other features to specific nitrogen moieties is uncertain at the present time. The −328 ppm peak occurs within the shift range of amines. The −119 ppm resonance could possibly be assigned to residual nitrile groups, and the peak at +19 ppm occurs in a chemical shift range typical of oxygen-bonded nitrogen species. Further work substantiating these assignments will be necessary. To this end, triple resonance $^{1}H-^{13}C-^{15}N$ solid-state NMR experiments are currently being undertaken.

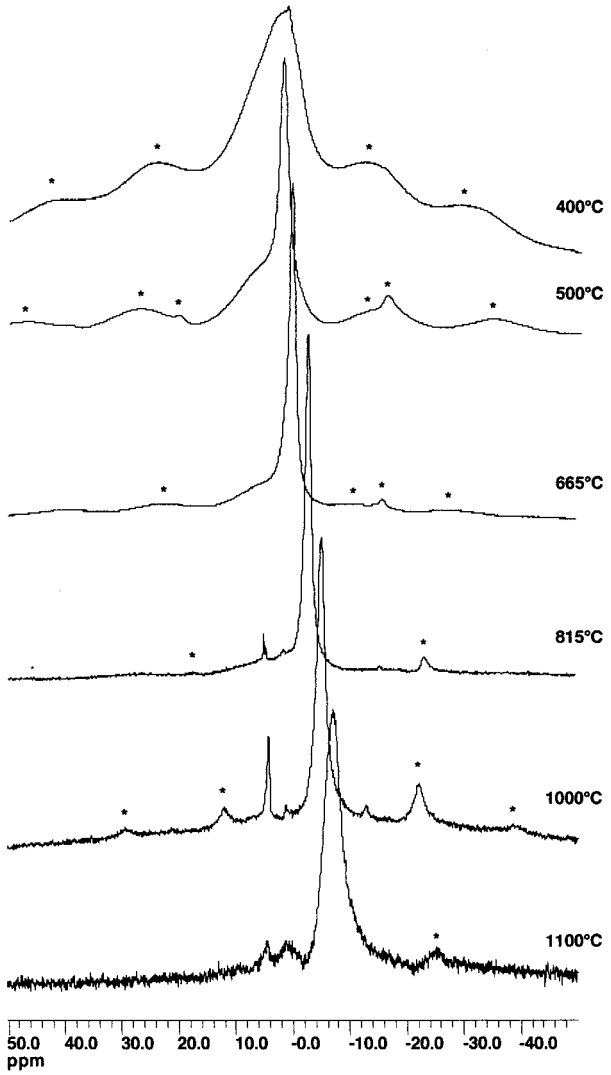

Figure 11. ^{1}H MAS of carbonized PMAN/DVB at various temperatures and times. Spinning sidebands are indicated by asterisks.

Figure 11 shows ^{1}H MAS NMR spectra as a function of increasing pyrolysis temperature of the carbons. The residual protons in the stabilized samples and even in the 500 °C pyrolysates give rise to broad indistinct line shapes with little chemical information. The widths of these peaks even under MAS conditions indicate significant dipolar broadening, suggesting the presence of domains in which the hydrogen-bearing species are segregated. In addition, for the thermally stabilized samples, a sharper resonance is observed near 2.0 ppm, which may arise from the carboxylic acid groups suspected to be present from the ^{13}C NMR results. This resonance is diminished toward higher pyrolysis temperatures, and a new, fairly sharp peak appears, which indicates the presence of motional averaging. As reported previously, amorphous carbon pyrolysates tend to sorb surface moisture from the atmosphere. TGA studies on the samples examined indicate that the water content under ambient conditions ranges between 0.5 and 7.5 wt %, with the higher pyrolysis temperatures being associated with larger weight losses below 200 °C. Assignment of these peaks to water molecules in contact with the pores is substantiated further by their near-

(22) Resing, H. A.; Weber, D. C.; Anderson, M.; Miller, G. R.; Moran, M.; Poranski, C. F.; Mattix, L. *ACS Polym. Prepr.* **1982**, *23*, 101.

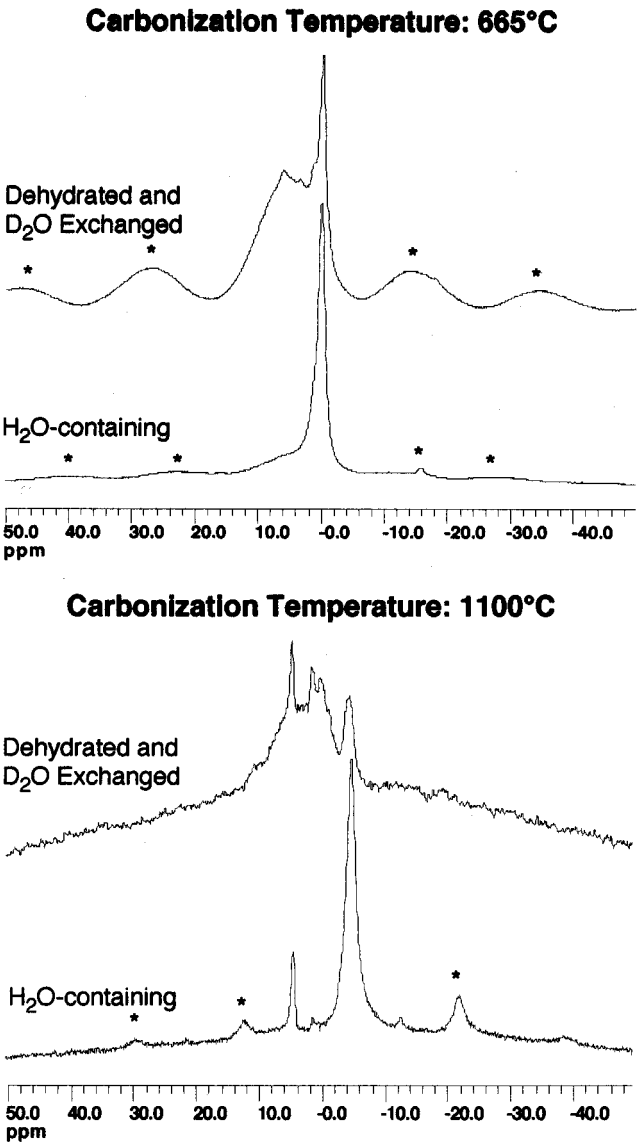

Figure 12. ^{1}H MAS of PMAN/DVB pyrolyzed at 665 °C (top) prior to and after D_2O exchange at the surface and at 1000 °C (bottom). Spinning sidebands are indicated by asterisks.

suppression in samples exchanged with D_2O vapor in a desiccator for 3 days (Figure 12).

The chemical environments sampled by these water molecules on the internal pore surfaces are sensitively reflected by the chemical shifts recorded in NMR measurements. In the present samples, these peaks shift linearly toward lower resonance frequencies as the pyrolysis temperatures are increased (Figure 13). For samples heated above 700 °C, they lie at significantly lower frequencies compared to the TMS reference standard. Negative chemical shift values for proton resonances have been observed previously for adsorbates on other carbonaceous materials, such as water on cokes,[23] xenon on grafoil,[24] and a variety of molecules adsorbed on the basal plane of graphitic carbon black.[25−27] Significant shift effects have also been observed for water on carbonized polyfurfurylaldehyde samples, where a direct correlation with the degree of carbonization was established.[11] Previous discussions

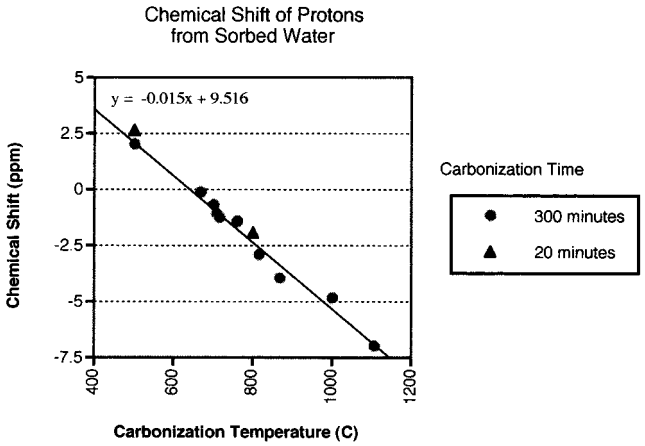

Figure 13. ^{1}H MAS chemical shifts of protons from sorbed water as a function of carbonization time and temperature.

have attributed the low-frequency shift to the fact that the molecules are adsorbed on the basal plane of the graphite surface where they experience a strongly diamagnetic component of the highly anisotropic magnetic susceptibility of the graphite structure.[28] Thus, the resonance of water was reported to shift to lower frequencies by ca. 15 ppm upon adsorption on crystalline graphite, while no significant shift is observed for water adsorbed on fully amorphous carbon black.[25] Following the above interpretation, we suggest that the low-frequency displacements seen for the samples in the present study reflect the degree to which pore near-surfaces resemble the regular polycyclic nature of a graphite surface. The ^{1}H NMR chemical shifts thus appear to be sensitive indicators of submicroscopic ordering processes that might be facilitated by the lack of constraint provided by free surfaces. Because the signals are motionally narrowed, only an average chemical environment is detected as the water molecules reorient on the surface, reorient within the pores, and/or diffuse in and out of the pores. It is important to note that, in contrast, atomic resolution TEM does not support any ordering which would extend more than 1−2 atomic layers into the solid. However, on the basis of the present experiments, the ^{1}H chemical shifts of the sorbed water molecules thus appear to be the most suitable NMR parameters for assessing the degree of local surface order in the present materials.

(4) Effects of Silicon Doping. According to Dahn et al., introduction of silicon-containing species into carbons prepared by chemical vapor deposition results in more favorable intercalation capacity.[29] The exact reasons for these observations are not well understood. Using the pyrolysis of polymeric precursors, silicon may also be introduced into the carbons by copolymerization with a suitable silane modifying agent. Solid-state NMR spectroscopy of ^{13}C and ^{29}Si is a well-suited technique for monitoring the fate of the silicon species at the various stages of the stabilization and carbonization process. ^{13}C CPMAS NMR spectra of untreated,

(23) Geschke, D. Z. *Phys. Chem.* **1968**, *239*, 138.
(24) Shibanuma, T.; Asada, H.; Ishi, S.; Matsui, T. *Jpn. J. Appl. Phys.* **1983**, *22* , 1656.
(25) Tabony, J. *Prog. NMR Spectrosc.* **1980**, *14*, 1.
(26) Tabony, J.; Bomchil, G.; Harris, N. M.; Leslie, M.; White, J. W.; Gamlen, P. H.; Thomas, R. K.; Trewern, T. D. *J. Chem. Soc., Faraday Trans. 1* **1979**, *75*, 1570.
(27) Tabony, J.; White, J. W.; Delachaume, J. C.; Coulon, M. *Surf. Sci. Lett.* **1980**, *95*, 282.
(28) Myers, K. J. *Molecular Magnetism and Magnetic Resonance Spectroscopy*; Prentice Hall: Upper Saddle River, NJ, 1973.
(29) Wilson, A. M.; Dahn, J. R. *J. Electrochem. Soc.* **1995**, *142*, 326.

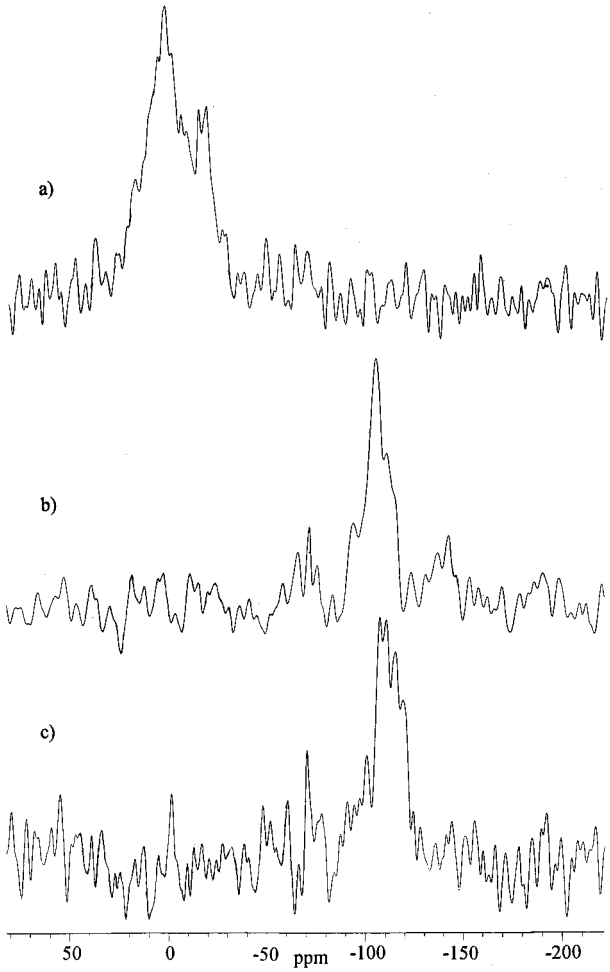

Figure 14. ^{29}Si CPMAS NMR spectra of PMAN/DVB/TVS: (a) untreated material; (b) oxidatively stabilized; (c) carbonized for 5 h at 500 °C.

oxidatively stabilized, and pyrolyzed carbons chemically modified by introduction of 1 mol % tetravinylsilane at the polymerization stage (9 wt % Si after pyrolysis) are virtually identical with those obtained on the analogous materials prepared and treated under the corresponding conditions in the absence of the silane additive. This gives us great confidence that the general PMAN/DVB structure has not undergone drastic organizational changes. Figure 14 shows the ^{29}Si CPMAS spectra and indicates dramatic changes in the bonding of the silicon species. The low signal-to-noise ratio is due to the low silicon content of these samples. The spectrum of the untreated copolymer is dominated by a broad resonance centered at 3 ppm, which can be assigned to carbon-bound silicon species linked to four alkyl groups. Additional contributions to the spectrum arise from silicon species linked to three alkyl and a terminal vinyl group (resonance contribution near −5 ppm), and silicon species linked to two alkyl and two terminal vinyl groups (feature near −15 ppm).

Figure 14b shows the spectrum following oxidative stabilization, indicating peaks in the −100 ppm range. A further displacement toward lower resonance frequencies (−110 ppm) is observed after pyrolysis at 500 °C (Figure 14c). Resonances at chemical shifts of −100 ppm and below are typical of silicon atoms in a tetrahedral oxygen environment. Thus, the NMR results indicate that the majority of the silicon species are being oxidized under the conditions of stabilization and pyrolysis. The small but significant shift of the resonances between the oxidatively stabilized and the pyrolyzed materials might indicate that the former sample contains a larger proportion of Si−O−C bonds, which are being replaced by Si−O−Si bonds upon pyrolysis at higher temperatures.

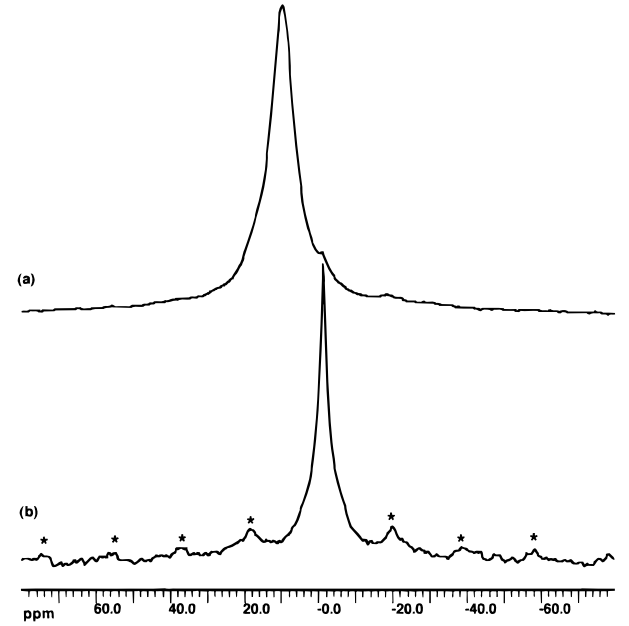

Figure 15. ^{7}Li MAS NMR spectra of lithium-intercalated PMAN/DVB, pyrolyzed at 700 °C for 5 h: (a) intercalated; (b) deintercalated. Spinning sidebands are indicated by asterisks.

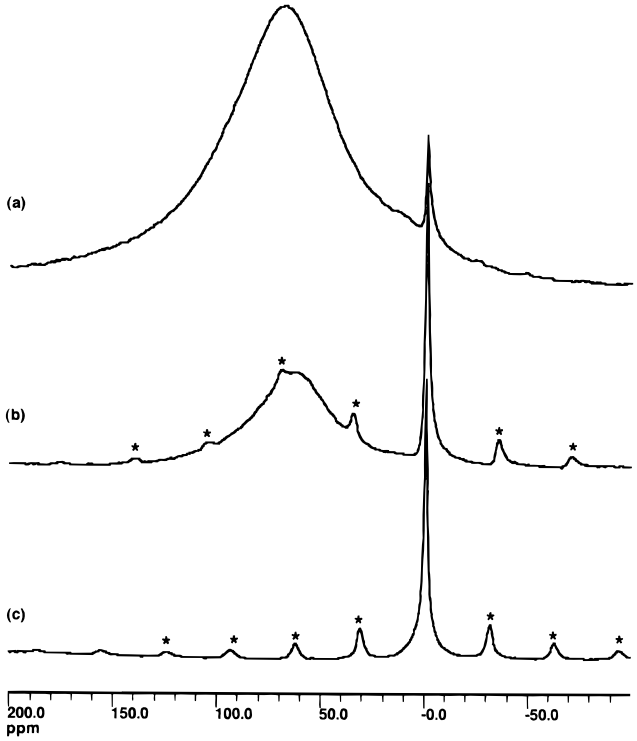

Figure 16. ^{7}Li MAS NMR spectra of lithium-intercalated PMAN/DVB, pyrolyzed at 1100 °C for 5 h: (a) intercalated, 1 s recycle delay; (b) intercalated, 30 s recycle delay; (c) deintercalated. Spinning sidebands are indicated by asterisks.

(5) Effects of Lithium Intercalation. Figures15 and 16 show ^{7}Li MAS NMR results on lithium-intercalated carbons, having previously undergone pyrolysis at 700 and 1100 °C, respectively. In both cases, fully intercalated as well as deintercalated samples are

shown, facilitating the distinction between reversibly and irreversibly generated lithium species. Clearly, three signal components are evident in the spectra. A very sharp line near −1 ppm is attributed to isotropically mobile lithium species in contact with the electrolyte solution that is wetting the surface. A broader line in the same chemical shift region, which also remains in the sample after deintercalation, is attributed to lithium species that are irreversibly removed from the electrochemical intercalation cycle by parasitic processes. The chemical shift suggests that this species is coordinated with oxygen as in LiOH or Li_2CO_3. Furthermore, the central resonance is flanked by a wide spinning sideband pattern, arising from resonance splitting due to first-order quadrupolar perturbations. A very similar peak pattern was recently observed in other types of lithiated amorphous carbons[9,13] and in ref 9 attributed to a Li_2 dimer species. We consider this assignment unlikely for our materials, because this resonance remains within fully deintercalated samples. Finally, both of the samples studied here show a dominant peak at the highest resonance frequencies, whose disappearance upon deintercalation supports the assignment to electrochemically relevant, intercalated species. The strong high-frequency shifts reflect sizeable unpaired spin density at the lithium sites from conduction electrons, as typically observed for metals and metal-like compounds ("Knight shift"). These results indicate that lithium ionization and transfer of charge to the carbon is far from complete. While our results are comparable to those obtained recently in other laboratories,[9,13] the wide range of ^{7}Li chemical shifts realized with the present class of amorphous carbons is particularly striking. To understand the large difference between these materials better, further NMR studies are in progress to eludicate the exact location of the lithium species. At the present time, review of our data and those available in the literature suggests that the magnitude of the chemical shift observed generally tends to increase with the pyrolysis temperature of the base carbons used; however, more systematic studies as a function of sample history are required. Figure 17 illustrates further that the ^{7}Li chemical shift is monotonically correlated with the total amount of charge transferred to the carbon during the intercalation process. This behavior is different from that of crystalline lithium graphite intercalates, where formation of second- and first-stage intercalation compounds is indicated by discontinous chemical shift changes.[12,30] The preliminary results obtained here so far suggest that beyond its utility for quantitatively discriminating between reversibly and irreversibly intercalated lithium species, ^{7}Li NMR might become a very useful tool for assessing and differentiating between various types of charging states in lithium insertion compounds of amorphous carbon materials.

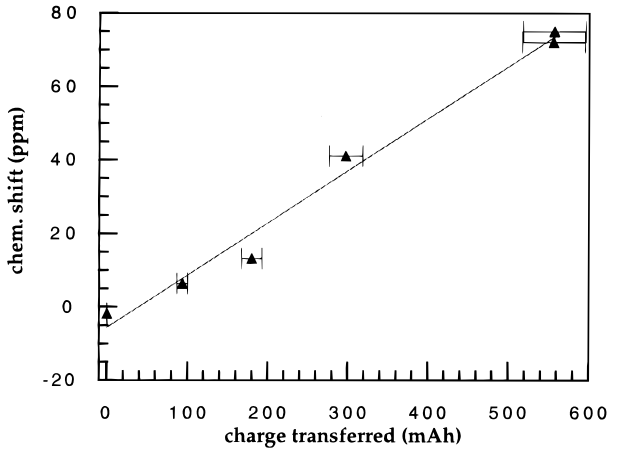

Figure 17. Correlation of ^{7}Li chemical shifts of lithium-intercalated PMAN/DVB, pyrolyzed at 1100 °C for 5 h, with the amount of charge transferred per gram during the intercalation process. Samples were cycled five times at 0.5 mA/cm^2 before intercalation at a charging rate of 0.25 mA/cm^2. The solid line is a linear least-squares fit to the data.

Conclusion

In conclusion, the results of the present study illustrate the utility of multinuclear solid-state NMR approaches for the structural analysis of amorphous carbon-based anode materials at various stages of their preparation and processing. While the present contribution gives only an overview, more detailed studies of specific preparation steps are underway, including the full range of structural tools besides solid-state NMR. The goal of these in-depth studies is to relate specific processing parameters to performance, via detailed structural information, and thereby aid in the development of preparation conditions that optimize the desired physical properties of these materials.

Acknowledgment. This study was supported by a grant from Sandia National Laboratories, Department of Energy Contract No. DE-AC04-94AL85000. We thank Marion Hunter and Tom Zifer at Sandia National Laboratories, Livermore, for providing the synthesis and some characterization of samples for this project. The ^{29}Si and ^{15}N NMR measurements were carried out with equipment sponsored by the National Science Foundation under the UCSB Materials Research Laboratory project. We thank Dr. Lucy Bull (Materials Research Laboratories), Michael Janicke (Department of Chemical Engineering, UCSB), and Luis Smith (Department of Chemistry, UCSB) for assistance with these measurements.

CM960389I

(30) Tatsumi, K.; Imamura, T; Zaghib, K.; Iwashita, N.; Higuchi, S.; Sawada, Y. *J. Electochem. Soc.* **1996**, *143*, 1923.